Journal of Nuclear Materials 386–388 (2009) 1006–1009

Contents lists available at ScienceDirect

Journal of Nuclear Materials

journal homepage: www.elsevier.com/locate/jnucmat

Surface electrical degradation due to ion bombardment of ITER insulators

S.M. Gonzalez de Vicente [a,*], A. Moroño [a], D.E. Hole [b], E.R. Hodgson [a]

[a] Euratom/CIEMAT Fusion Association, Avenida, Complutense 22, 28040 Madrid, Spain
[b] University of Sussex, Science and Technology, Brighton BN1 9QH, UK

A B S T R A C T

Insulators will be used in ITER diagnostic systems where they will play an important role for optical components, as well as in neutral beam injector system. In addition to neutron and gamma radiation, these materials will be subjected to bombardment by low energy ions and neutral particles. Previous works carried out in silica have shown a dramatic surface electrical and optical degradation with a marked temperature dependence when the material is subjected to proton or alpha particle bombardment, due to loss of oxygen from the surface caused by preferential sputtering by energetic ions. Therefore, it was necessary to extend the study to the main candidate ceramic insulators for ITER (alumina, BeO and AlN), in order to evaluate possible issues for both diagnostic and heating and current driven systems. A clear optical and electrical degradation have been found in all the materials studied after implantation, in general this appears to be an issue common to all the insulator materials studied. This degradation is related with oxygen loss from the implanted zone for alumina and BeO, as observed previously for silica, and nitrogen loss for AlN. For silica implanted at higher energies data show surface degradation in all cases again due to loss of oxygen with a markedly different behaviour for each implanted ion.

1. Introduction

Insulator materials will be extensively used in ITER in heating and current drive, and diagnostic systems where they will play important roles as electrical insulators, and RF and optical transmission components. These materials will be subjected to neutron and gamma radiation, and additionally to bombardment by low energy ions and neutral particles of energies between eV and keV as a consequence of neutron reactions and related sputtering at vacuum surfaces, as well as ionization and acceleration of the residual gas due to local electric fields. Low energy particles deposit most of their energy at or very near the surface, producing high levels of ionization, atomic displacement, and sputtering. Hence, the resulting local damage and consequent degradation of the physical properties at the vacuum surface could be high. In particular, optical transmission and electrical resistivity are important properties for heating and current drive, and diagnostic system applications. Such potential degradation needs to be assessed in detail.

The main candidate ceramic insulators for ITER are KS-4V, alumina, BeO and AlN. In previous work severe electrical and optical degradation for proton (H) and helium implanted KS-4V due to oxygen loss produced by radiolitic sputtering has been reported [1–3]. The aim of the work presented here is to assess the behaviour of the different insulators for ITER in the same way as for KS-4V, in order to evaluate possible issues for both diagnostic, and heating and current driven systems. Also, as a particular case for NBI, to extend the study to higher energies.

2. Experimental procedure

KS-4V (SiO_2 quartz glass), sapphire, BeO, and AlN samples of approximately $10 \times 10 \times 0.8\ mm^3$ were cut and in the case of KS-4V and sapphire optically polished. Samples were mounted on a small oven in the CIEMAT Danfysik 60 kV ion implanter beam line chamber. The system allows temperature control from about 20–600 °C during implantation in high vacuum ($\approx 5 \times 10^{-6}$ mbar). Two platinum electrodes separated by 1.5 mm were sputtered onto the sample face to be implanted and DC surface electrical conductivity with a current sensitivity of 10^{-11} A may be measured by applying 100 V between the electrodes. In this way samples have been implanted with 54 keV He^+ ions at 50 °C, 0.5 mA/cm^2 up to a dose of 2×10^{17} ions/cm^2, and the surface conductivity measured.

KS-4V samples were similarly mounted on an oven in the Sussex University 3.0 MeV Van de Graaff accelerator. This system allows temperature control from about 20–80 °C during implantation in high vacuum. The measurement system was the same as at CIEMAT Ion Implanter. Samples were implanted with 900 keV He^+ ions at 50 °C, 0.5 mA/cm^2 up to a dose of 2×10^{17} ions/cm^2; and 300 and 900 keV H^+ ions at 50 °C, 0.5 mA/cm^2 up to a dose of 2×10^{17} ions/cm^2, and the surface conductivity measured.

* Corresponding author. Tel.: +34 91 346 6204; fax: +34 91 346 6124.
E-mail address: sgdvicen@sckcen.be (S.M. Gonzalez de Vicente).

0022-3115/$ - see front matter © 2009 Elsevier B.V. All rights reserved.
doi:10.1016/j.jnucmat.2008.12.200

Optical absorption measurements from 195 to 3000 nm were performed on KS-4V and sapphire samples before and after implantation, with a Varian Cary 5 spectrometer, as well as SEM X-ray analysis on KS-4V, sapphire, and AlN with an Hitachi S-2500 scanning electron microscope.

3. Results

Fig. 1 shows the surface electrical current as a function of ion dose for SiO_2, Al_2O_3, BeO, and AlN samples implanted with He^+ ions, at 50 °C. For all the samples, the surface current is at or below the measuring limit (10^{-11}A) up to a dose of about 4×10^{15} ions/cm^2, after which a nearly exponential current increase with dose is observed, and begins to saturate by about 4×10^{16} ions/cm^2. For SiO_2 and Al_2O_3 the observed saturation is more rapid, and the measured surface current is one order of magnitude lower than for BeO and AlN. In Fig. 2, the induced optical absorption for the SiO_2 and Al_2O_3 implanted samples are given. The absorption increase is monotonic for decreasing wavelength in both cases.

The SEM X-ray analyses for unimplanted and implanted Al_2O_3 and AlN samples at 50 °C are shown in Fig. 3. The aluminium and oxygen peaks are clearly identified, whereas nitrogen peak can hardly be measured as it is at the lower limit of measurement. In case of Al_2O_3, the proportion of oxygen is reduced by 80% or more after implantation. For AlN it is possible to observe a significant reduction of the nitrogen after implantation, as may be seen in the inset.

Fig. 4 shows the surface electrical current as a function of ion dose for SiO_2 samples implanted with He^+ and H^+ ions, at different energies. Alpha particles were implanted at 27, 54 and 300 keV, at 50 °C. In this case, the surface current is at or below the measuring limit (10^{-11} A) up to a dose of about 7×10^{16} ions/cm^2 for the sample implanted at 27 keV, whereas for samples implanted at higher energies (54 and 300 keV) it is 5×10^{-11} A, due to ionic conductivity enhanced by the beam heating the sample. For the 27 keV implanted sample a nearly exponential current increase with dose is observed, and by about 3×10^{16} ions/cm^2 the current increase begins to saturate. The same behaviour is observed for 54 and 300 keV implanted samples, but in these cases, the current increase begins to saturate by about 5×10^{16} and 10^{17} ions/cm^2, respectively. The induced optical absorption for the three different implantation energies for He^+ implanted samples is given in Fig. 5. The absorption increase is monotonic for decreasing wavelength

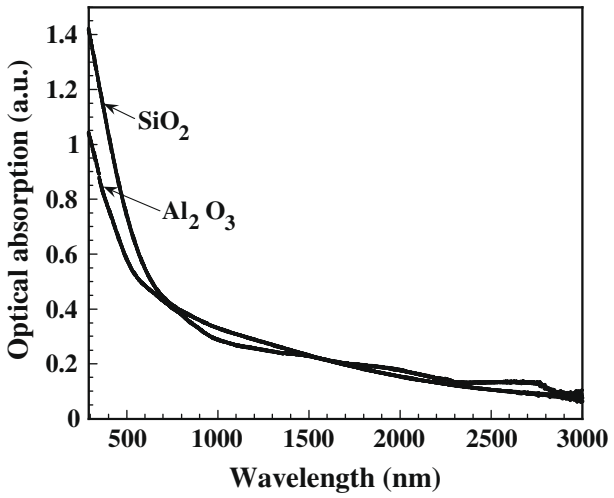

Fig. 2. Optical absorption spectra for SiO_2 and Al_2O_3 samples implanted with He^+, at 50 °C up to a dose of 10^{17} ions.

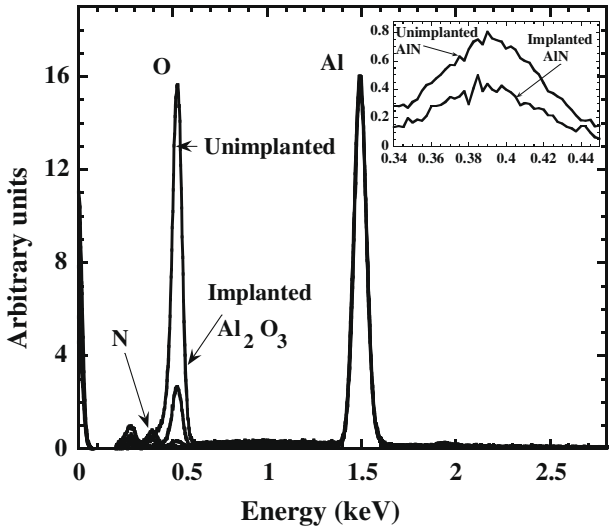

Fig. 3. SEM X-ray analysis for both the unimplanted and implanted zone of Al_2O_3 and AlN samples He^+ implanted at 54 keV and 50 °C.

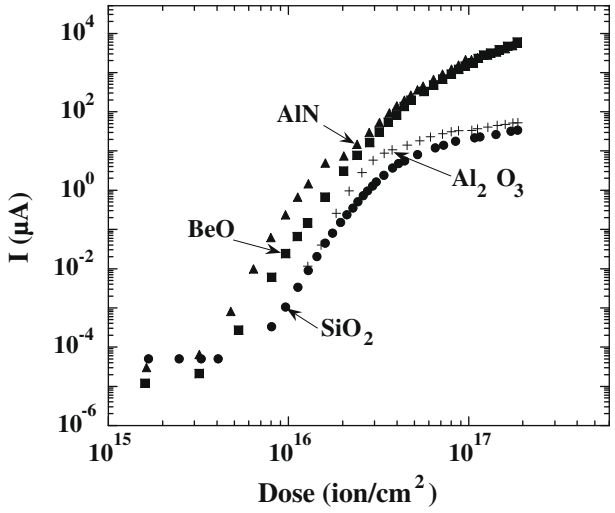

Fig. 1. Surface electrical current as a function of ion dose for different He^+ implanted samples (SiO_2, Al_2O_3, BeO and AlN), at 50 °C.

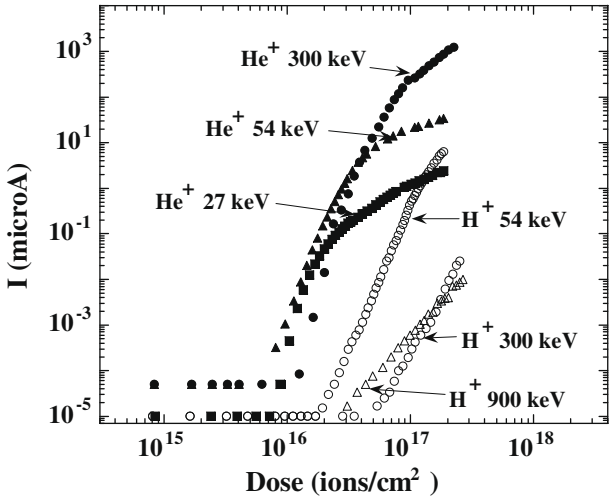

Fig. 4. Surface electrical current as a function of ion dose for SiO_2 samples implanted with He^+ at 27, 54 and 300 keV, and H^+ at 54, 300 and 900 keV, at 50 °C.

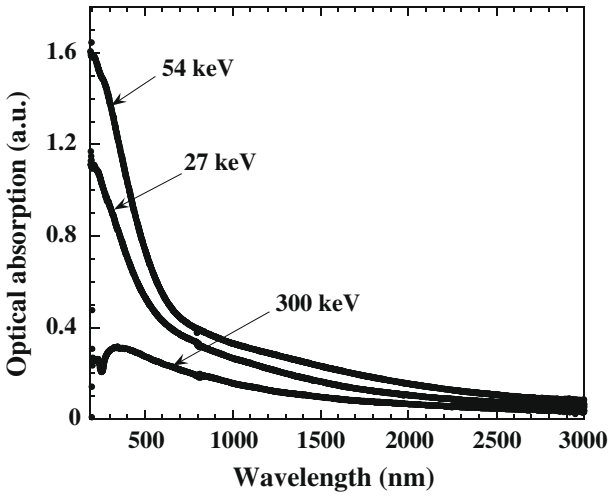

Fig. 5. Optical absorption spectra for SiO_2 samples implanted with He^+ at different energies: 27, 54 and 300 keV, at 50 °C up to a dose of 10^{17} ions.

for all three energies, but the optical degradation markedly decreases with increasing implantation energy.

Implantations with protons at 54, 300 and 900 keV, at 50 °C on SiO_2 samples are shown in Fig. 4. Surface electrical degradation was measured at lower doses for lower implantation energies. Thus, the current remained at or below the measure limit up to a dose of about 2×10^{16}, 3×10^{16}, and 4×10^{16} ions/cm^2 for proton implantations carried out at 54, 900 and 300 keV, respectively. After that, a nearly exponential current increase with dose is observed in all three energies. No saturation of the current increase was seen for any energy, although marked differences between high (300 and 900 keV) and low (54 keV) energy implanted samples were found. Electrical degradation for the low energy implanted sample is almost four orders of magnitude higher than at high energy.

The induced optical absorption for the three different energies for H^+ implanted samples is given in Fig. 6. The absorption increase is monotonic for decreasing wavelength for all three energies, the optical degradation slightly increases with increasing implantation energy up to a wavelength of around 315 nm. From 315 nm to 290 nm, optical absorption is higher for 54 keV implanted samples.

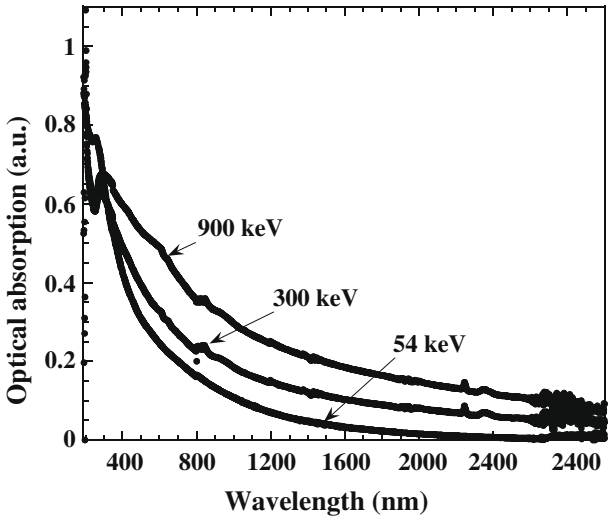

Fig. 6. Optical absorption spectra for SiO_2 samples implanted with H^+ at different energies: 54, 300 and 900 keV, at 50 °C up to a dose of 10^{17} ions.

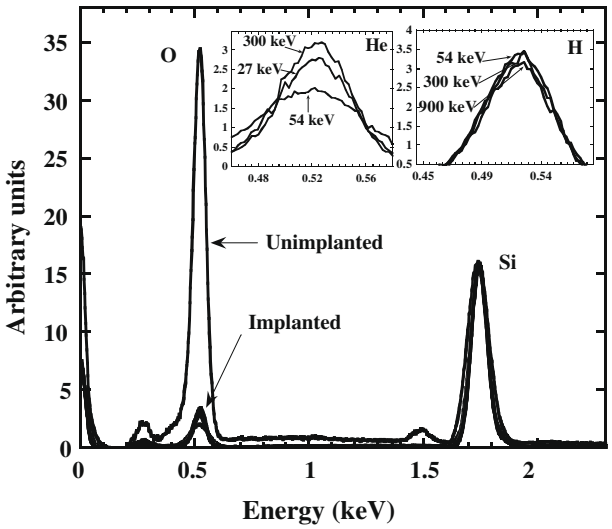

Fig. 7. SEM X-ray analysis for both the unimplanted and implanted zone of SiO_2 samples implanted with He^+ at 27, 54 and 300 keV, and H^+ at 54, 300 and 900 keV, at 50 °C.

In Fig. 7 the SEM X-ray analyses for unimplanted and implanted KS-4V samples at 50 °C are shown. Samples have been implanted with alpha particles at 27, 54 y 300 keV, and with protons with 54, 300 and 900 keV. In all the cases, a dramatic oxygen reduction is observed. Details of oxygen peaks for implanted samples can be seen in the insets.

4. Discussion

Sapphire, BeO and AlN surface degradation after He^+ implantation, characterized by high electrical conductivity and enhanced optical absorption, is similar to that observed previously in silica (Figs. 1 and 2) [1–3]. The main reason for the surface degradation reported here is oxygen preferential sputtering for sapphire and beryllia, and nitrogen preferential sputtering for AlN, as one can see in Fig. 3, i.e. preferential sputtering of the most electronegative ion of the compound. As result of this degradation, the material surface behaviour is more like a semiconductor than an insulator, with an increase in surface electrical conductivity after implantation between five and nine orders of magnitude.

To study surface opto-electrical degradation dependence on implanted ion energy, silica samples were implanted with He at 27, 54 and 300 keV and protons at 54, 300 and 900 keV. In all materials, after implantation, severe degradation was found. He implanted samples at higher energies exhibit a higher electrical degradation (Fig. 4). The main parameter to explain this phenomenon is the electronic ion stopping power (dE/dx), the rate of energy deposition by the ion via electronic interactions with the material. Samples implanted with He^+ at 27 and 54 keV show a higher oxygen reduction (Fig. 7), i.e. higher structural damage. This

Table 1
Electronic stopping power for He^+ and H^+ ions implanted into SiO_2 at different energies. Simulation carried out with SRIM 2006 [8].

Ion	Energy (keV)	$\frac{dE}{dx_{elec}}$ (keV/μm)
He^+	27	96.9
	54	142.8
	300	317.3
H^+	54	125.1
	300	86.4
	900	46.8

large oxygen reduction implies that the surface region must contain substantial amounts of SiO_x with $2 < x < 0$, and Si rich zones due to such a high concentration of oxygen vacancies. For 300 keV He stopping power is higher, and electronic excitation extends further from the surface, as one can see in Table 1. Oxygen vacancies produced in the surface region can more easily migrate into the bulk [4,5], and hence cause less structural modification. At higher implantation energies the density of oxygen vacancies in the near surface region will be less, giving rise to less SiO and hence band gap reduction and related sputtering yield will be less. This is in agreement with the X-ray SEM analysis where the apparent oxygen reduction is less for higher energies, and the optical absorption for 300 keV implanted samples shows much less SiO absorption (Fig. 5). The electrical degradation does not correlate with the optical degradation nor with the apparent oxygen reduction, it must therefore be related to the number of isolated oxygen vacancies which at higher electronic excitation are produced at a higher rate and are distributed over a larger surface volume.

For proton implanted samples, a different behaviour is observed. Electrical degradation is higher for lower energies (Fig. 4). In contrast to He, electronic stopping power for protons decreases for higher energies (Table 1). For proton implantations as the electronic stopping power is less, a higher dose is necessary to degrade the sample and reach saturation. Optical degradation is higher for 27 an 54 keV He^+ than for H^+, and in case of protons, higher optical degradation corresponds to higher energy (Fig. 6). Again the degradation is related with a significant loss of oxygen from the material surface (Fig. 7), increasing for higher energies.

Although there are differences, for H^+ and He^+, the same electrical characteristics have been found. Surface electrical degradation appears, with an increase in conductivity between one and nine orders of magnitude depending on the ion and energy.

The surface electrical and optical degradation reported here is an issue for both ITER and future fusion reactors where electrical insulators will be subjected to bombardment by low energy ions and neutral particles of energies between eV and keV as a consequence of neutron reactions and related sputtering at vacuum surfaces, and ionization and acceleration of the residual gas due to local electric fields. The flux and energy of the residual gas ions will be function of pressure, electric field, and gamma radiation levels. Work is under way in order to assess the realistic particle spectrum and flux due to residual gas ionization [6,7].

5. Conclusions

Ion bombardment produces severe electrical and optical degradation in all the insulator materials studied and appears to be a common issue. This may prove to be a serious technological issue for ITER and future fusion reactors. The observed degradation needs to be fully examined to assess the relevance for ITER.

Acknowledgements

KS-4V was kindly provided by the Russian Federation as part of the EU-RF ITER collaboration. The authors wish to thank F.J. Valle Paisán and A. Muñoz Lázaro for their help with these experiments. This work, supported by the European Communities under the contract of Association between EURATOM and CIEMAT was carried out within the framework of the European Fusion Development Agreement. The views and opinions expressed herein do not necessarily reflect those of the European Commission. It has also been partly financed by the Spanish Ministry of Science and Technology (FTN2003-03855).

References

[1] S.M. González, A. Moroño, E.R. Hodgson, 74 (2005) 831.
[2] S.M. González, A. Moroño, E.R. Hodgson, J. Nucl. Mater. 367–370 (2007) 1014.
[3] S.M. González de Vicente, A. Moroño, E.R. Hodgson, Fus. Eng. and Design 82 (2007) 2567.
[4] N. Itoh, M. Stoneham, Materials Modification by Electronic Excitation, Cambridge University Press, 2001.
[5] V.A. Starostin, Nuclear Instruments and Methods in Physics Research Section B: Beam Interactions with Materials and Atoms, 242, Issues 1–2, p. 402. Ion Beam Modification of Materials - Proceedings of the 14th International Conference on Ion Beam Modification of Materials, (2006).
[6] E.R. Hodgson, A. Moroño, S.M. González de Vicente, Fus. Eng. and Design 82 (2007) 2578.
[7] E.R. Hodgson, A. Moroño, S.M. González de Vicente, J. Nucl. Mater. 386–388 (2009) 999.
[8] J.F. Ziegler, J.P. Boersack, U. Littmark (Eds.), The Stopping and Ranges of Ions in Solids, Pergamon, New York, 1985. (see also the SRIM web page <http://www.srim.org>).